ROD TORSION IN KINEMATIC CREEP MODES

I. A. Bashchikova*

UDC 539.376

Abstract: Problems that describe the shaping of a residual twist angle to a rod under creep conditions with account for elastic recovery after unloading are considered. It is assumed that a constant linear twist angle is set for the section being formed, i.e., the section is under pure torsion conditions with no constraints to the ends of the rod. It is stated that strains and stresses depend only on time and two spatial coordinates in the cross-sectional plane of the rod. Direct and inverse problems of torsion of rectangular and angular rods in various kinematic creep modes are considered. The twist angle rate during the entire deformation process is set to be constant. An approach is proposed for the numerical calculation based on the finite element method, which makes it possible to obtain the stiffness characteristics of the section under torsion in the case of creep. It is shown that the minimum level of residual stresses is observed during relaxation deformation. The modes in which stresses significantly decrease in their concentration region are determined for a corner-type rod.

Keywords: torsion, rod, cross-sectional warping, kinematic modes, creep, inverse problem.

INTRODUCTION

Corner-shaped, T-shaped, rectangular, and other types of profiles are widely used as reinforcing elements in hull plating, aircrafts, shipbuilding, and general engineering products. The length of such profiles can reach several meters, the twist angle usually does not exceed 0.5 rad/m, and the curvature of the curved axis of the profile is not larger than 0.5 m^{-1}. The characteristic cross-sectional dimensions (wall height and flange height of corner- and T-shaped profiles) are approximately several centimeters, and the cross-sectional thickness is usually a few millimeters. The manufacture of parts under rapid plastic deformation conditions often leads to fracture of the structure even during the production stage. For example, flanges can detach at normal temperature when corner- or T-shaped profiles are bent using rolling mills consisting of a system of roller blocks and designed to create such profiles. This phenomenon is explained by high stress concentration in the flange joint region and sharp changes in the geometric shape of the cross section. One of the ways to create the desired geometry of these profiles is the sequential shaping of their sections in a heat chamber under slow conditions, in which case most irreversible deformations are creep strains. It can be assumed that, within the molded section of the profile (rod) located in the furnace, there is no constraint at the ends of the rod and the linear twist angle along with the curvature of the curved axis of the profile reaches constant values. The twist angle is understood as the cross-sectional angle of rotation of the rod per unit length. After the completion of the molding and unloading processes, elastic recovery is possible due to the large difference in the cross-sectional length and dimensions of the section. Similar direct and inverse problems pertaining to the shaping of plates and profiles are considered in [1–5].

Lavrentyev Institute of Hydrodynamics, Siberian Branch, Russian Academy of Sciences, Novosibirsk, 630090 Russia; *binna@ngs.ru.
*Corresponding author.

This paper presents the study of direct and inverse problems of pure torsion with no constraints on the ends of rectangular and corner-shaped rods in creep modes in the case where the twist angle rate is considered to be set during the entire deformation process. Determining the stress–strain state in a corner-shaped cross section is complicated by the presence of a stress concentration region. As there is no constraint on the ends, the problem may be stated in a two-dimensional formulation. It is proposed to solve the problem numerically using a calculation technique based on the finite element method. Similar two-dimensional problems of rod torsion under creep conditions are described in [1] using the finite difference method. However, the use of this method significantly complicates the description of the cross-sectional geometry of a profile of a complex shape, as well as the approximation of the boundary conditions.

1. FORMULATION OF DIRECT AND INVERSE PROBLEMS OF TORSION

The problems are formulated and the resolving equations are written down the following way.

1.1. Direct Problem of Torsion

At an initial time $t = 0$, the rod under the action of torque is deformed elastically up to a given linear twist angle θ_0. The twist angle rate $\dot{\theta} = \text{const}$ is assumed to be known within a time range $0 \leqslant t < t_*$, and deformation relaxation also becomes possible, in which case the angle remains the same: $\dot{\theta} = 0$. Irreversible creep strains accumulate in the rod. Now the goal is to determine the residual twist angle θ_{**} after elastic recovery at $t = t_*$ due to unloading (time t_* is given).

1.2. Inverse Problem of Torsion

The task is to calculate the initial twist angle θ_0 by which the rod should be elastically deformed at an initial time $t = 0$ in order to obtain the given residual twist angle θ_{**} after deforming it during a time range $0 \leqslant t < t_*$ at a given twist rate $\dot{\theta} = \text{const}$ and elastic unloading at $t = t_*$.

At $0 \leqslant t \leqslant t_*$, the temperature is assumed to be constant; at $t < 0$, the rod is not deformed. The solution to the inverse problem can be obtained by the method of successive approximations, solving the direct problem at each step and using an iterative process similar to that described in [1, 2].

Let the z axis be directed along the rod. Let the x and y axes be located in the cross-sectional plane. As there is no constraint on the ends of the rod, the angle of rotation per unit length $\theta = \theta(t)$ does not depend on the z coordinate and section z rotates relative to the section $z = 0$ by the twist angle $\varphi = \theta z$. Then, the following dependences are written for the displacements [6]:

$$u = -\varphi y = -\theta z y, \qquad v = \varphi x = \theta z x, \qquad w = W(x, y, t). \tag{1}$$

Here $W = W(x, y, t)$ denotes the displacement of the cross-sectional points of the rod in the z direction, which occurs during torsion (warping of the section). Strains $\gamma_{zx} = \gamma_{zx}(x, y, t)$ and $\gamma_{zy} = \gamma_{zy}(x, y, t)$ are determined from the Cauchy relations. In view of Eq. (1), the following can be written provided that $t = 0$:

$$\gamma_{zx}(x, y, 0) = \gamma_{zx0} = W_{0,x} - \theta_0 y, \qquad \gamma_{zy}(x, y, 0) = \gamma_{zy0} = W_{0,y} + \theta_0 x. \tag{2}$$

Here $\theta_0 = \theta(0)$ and $W_0 = W(x, y, 0)$. At $t = 0$, stresses $\tau_{zx} = \tau_{zx}(x, y, t)$ and $\tau_{zy} = \tau_{zy}(x, y, t)$ are related to strains (1) by Hooke's law

$$\tau_{zx}(x, y, 0) = \tau_{zx0} = G\gamma_{zx0}, \qquad \tau_{zy}(x, y, 0) = \tau_{zy0} = G\gamma_{zy0}, \tag{3}$$

where G is the shear modulus. Stresses (3) satisfy the equilibrium equation

$$\tau_{zx0,x} + \tau_{zy0,y} = 0 \tag{4}$$

with boundary conditions on the cross-sectional contour

$$\tau_{zx0}n_x + \tau_{zy0}n_y = 0 \tag{5}$$

892

(n_x and n_y are the components of the normal to the contour). The initial torque is

$$M_{z0} = \int_S (\tau_{zy0}x - \tau_{zx0}y)\,dS = \theta_0 D, \qquad (6)$$

where D is the stiffness of the rod section under elastic torsion and S is the cross-sectional area of the rod.

It is assumed that, at any time $0 \leqslant t < t_*$, the total strains are the sum of elastic strains and creep strains, which means that, in view of Eq. (2), the following can be written:

$$\frac{1}{G}\dot{\tau}_{zx} + \eta_{zx}^c = \dot{W}_{,x} - \dot{\theta}y, \qquad \frac{1}{G}\dot{\tau}_{zy} + \eta_{zy}^c = \dot{W}_{,y} + \dot{\theta}x \qquad (7)$$

(η^c is the creep strain rates). The creep of the material is described by the kinetic theory, taking into account the damage accumulation [7]:

$$\eta_{kl}^c = \frac{1}{(1-\omega)^m}\frac{3}{2}\frac{f_1(\sigma_i)}{\sigma_i}\sigma_{kl}^0, \qquad \dot{\omega} = \frac{f_2(\sigma_i)}{(1-\omega)^m}. \qquad (8)$$

Here $\sigma_i = (3\sigma_{kl}^0\sigma_{kl}^0/2)^{1/2}$ is the stress intensity, σ_{kl}^0 is the stress deviator components, and $0 \leqslant \omega \leqslant 1$ is the damage parameter. In this case, $\sigma_i = (3\tau_{zx}^2 + 3\tau_{zy}^2)^{1/2}$. At $0 \leqslant t < t_*$, Eqs. (4) and (5) for stress rates yield

$$\dot{\tau}_{zx,x} + \dot{\tau}_{zy,y} = 0; \qquad (9)$$

$$\dot{\tau}_{zx}n_x + \dot{\tau}_{zy}n_y = 0. \qquad (10)$$

Torque in the cross section of the rod is determined as

$$M_z = \int_s (\tau_{zy}x - \tau_{zx}y)\,ds. \qquad (11)$$

Equations (7)–(11) represent a differential system, and one can determine the stress–strain state at $0 \leqslant t < t_*$ by solving this system under the initial conditions W_0, τ_{zx0}, and τ_{zy0}.

At $t = t_*$ the rod is unloaded elastically. The stress equations before unloading $\tau_{zx*} = \tau_{zx}(x, y, t_*)$ and $\tau_{zy*} = \tau_{zy}(x, y, t_*)$ can be represented as

$$\tau_{zx*} = \tau_{zx}^e + \rho_{zx}, \qquad \tau_{zy*} = \tau_{zy}^e + \rho_{zy}, \qquad (12)$$

where ρ_{zx} and ρ_{zy} are the residual stresses and τ_{zx}^e and τ_{zy}^e are the stresses corresponding to elastic recovery.

The equation of elastic unloading has the following form:

$$\int_s (\tau_{zy*}x - \tau_{zx*}y)\,ds = \theta^e D$$

(θ^e is the angle at which elastic recovery occurs).

Due to the problem formulation, $\dot{\theta} = \text{const}$. The following is written for the residual twist angle:

$$\theta_{**} = \theta_* - \theta^e = \theta_0 + \dot{\theta}t_* - \theta^e. \qquad (13)$$

Solutions to the inverse problem can be obtained using the iterative process

$$\theta_0^{k+1} = \theta_0^k + (\theta_{**} - \theta_{**}^k). \qquad (14)$$

Here θ_0^k and θ_{**}^k are the initial twist angle and the residual twist angle, respectively, which are obtained by solving the direct problem at iteration k. The equality $\theta_0^1 = \theta_{**}$ can be chosen as a first approximation. The problem of convergence of similar iterative processes in solving inverse problems is studied in [5].

2. NUMERICAL SOLUTION METHODS

If the section contains singular points at which stress concentration occurs, the application of the finite difference method [1] is difficult. The calculations are carried out using the finite element method based on the displacement variation method and proposed for solving the torsion problems in [6]. As displacements are varied in Eq. (1), the following is obtained:

$$\delta u = 0, \qquad \delta v = 0, \qquad \delta w = \delta W(x, y, t).$$

As the possible work of external forces (torque) vanishes at an initial time $t = 0$, the work of internal forces vanishes too:

$$\int_S (\tau_{zx0}\, \delta\gamma_{zx0} + \tau_{zy0}\, \delta\gamma_{zy0})\, dS = 0. \tag{15}$$

In view of Eqs. (2) and (3) and the fact that the strain variation is $\delta\gamma_{zx0} = (\delta W_0)_{,x}$ and $\delta\gamma_{zy0} = (\delta W_0)_{,y}$, integral (15) is transformed into

$$\int_S (W_{0,x} - \theta_0 y)(\delta W_0)_{,x} + (W_{0,y} + \theta_0 x)(\delta W_0)_{,y}\, dS = 0. \tag{16}$$

The cross-sectional area is partitioned into triangular finite elements. Inside element p, the desired warping function $W_0(x, y)$ is represented as

$$W_0^p = (N)(W_0^p), \tag{17}$$

where $(N) = (N_1, N_2, N_3)$ is the shape function vector and $(W_0^p) = (W_0^{p_1}, W_0^{p_2}, W_0^{p_3})^{\mathrm{t}}$ is the vector of the warp function values at three nodes of the element. With account for Eq. (17), expression (16) is transformed into the following system of linear equations:

$$[R_{ij}^p](W_0^{p_i}) = (F_i^p), \qquad i = 1, 2, 3,$$

$$[R_{ij}^p] = \int_s \left(\frac{\partial N_i}{\partial x} \frac{\partial N_j}{\partial x} + \frac{\partial N_i}{\partial y} \frac{\partial N_j}{\partial y} \right) ds, \qquad (F_i^p) = \int_s \left(\theta_0 y \frac{\partial N_i}{\partial x} - \theta_0 x \frac{\partial N_i}{\partial y} \right) ds. \tag{18}$$

Here superscript p corresponds to element p and $[R^p]$ denotes the stiffness matrix of element p. The shape functions are equated to the L coordinates of the triangle $N_i = L_i$ $(i = 1, 2, 3)$, where

$$L_1 = \frac{1}{2s}(a_1 + b_1 x + c_1 y), \quad L_2 = \frac{1}{2s}(a_2 + b_2 x + c_2 y), \quad L_3 = \frac{1}{2s}(a_3 + b_3 x + c_3 y). \tag{19}$$

Here $a_1 = x_2 y_3 - x_3 y_2$, $b_1 = y_2 - y_3$, and $c_1 = x_3 - x_2$ (the remaining coefficients are obtained by the circular permutation of the superscripts); x_i and y_i are the coordinates of the element nodes in the Cartesian coordinate system; s is the area of the considered element p:

$$s = \frac{1}{2} \det \begin{vmatrix} 1 & x_1 & y_1 \\ 1 & x_2 & y_2 \\ 1 & x_3 & y_3 \end{vmatrix}.$$

Thus, the warping inside the element has a linear approximation $W_0^p = (L_1, L_2, L_3)(W_0^p)$. It is noteworthy that a more complex nonlinear approximation for W_0^p [8] can also be used, but this could complicate the numerical integration. In the case of linear functions, a satisfactory computational accuracy is achieved by partition of the section into smaller finite elements.

After Eq. (19) is substituted into system (18), the latter can be represented as

$$[R^p](W_0^p) = (F^p) \tag{20}$$

Here $[R^p] = s[B^p]^{\mathrm{t}}[B^p]$ is the stiffness matrix of the element and $(F^p) = \theta_0 s[B^p]^{\mathrm{t}}(y_s, -x_s)^{\mathrm{t}}$, where

$$[B^p] = \frac{1}{2s} \begin{bmatrix} b_1 & b_2 & b_3 \\ c_1 & c_2 & c_3 \end{bmatrix}, \qquad x_s = \frac{x_1 + x_2 + x_3}{3}, \qquad y_s = \frac{y_1 + y_2 + y_3}{3}.$$

Integration (18) is performed approximately using the following equations from [8, 9]:

$$\int_s \phi(x, y)\, ds = 2s \int_0^1 \int_0^{1-L_1} \phi(L_1, L_2, L_3)\, dL_2\, dL_1 = s \sum_{r=1}^J d_r \phi(L_{1r}, L_{2r}, L_{3r})$$

[J is the number of integration points; d_r and $\phi(L_{1r}, L_{2r}, L_{3r})$ are the weight coefficients and the value of function ϕ at the integration point r]. In this case, $J = 1$, the integration point has coordinates $L_1 = L_2 = L_3 = 1/3$ and the weight coefficient is equal to $d = 1$. After system (20) is obtained for each element, the stiffness matrix $[R]$

894

and vector (F) are calculated for the entire element system of the section. As a result, the following system of linear equations is obtained:

$$[R](W_0) = (F). \tag{21}$$

Here $(W_0) = (W_0^1, W_0^2, \ldots, W_0^{m_1})$ is the desired vector and m_1 is the number of nodes of the system. Strains (2) are determined via the resulting values of (W_0) as follows:

$$(\gamma_{zx0}, \gamma_{zy0})_p^{\mathrm{t}} = [B^p](W_0^p) + \theta_0(-y_s, x_s)_p^{\mathrm{t}}.$$

Then, stresses (3) are calculated at the center of gravity of each element, after which the total moment M_{z0} is determined [by replacing the integral (6) with the sum of all moments calculated for each element], as well as the stiffness of the rod $D = M_{z0}/\theta_0$. Thus, when solving the direct problem of the rod torsion, all values at an initial time $t = 0$ become known.

At $0 \leqslant t < t_*$, system (7)–(11) with the initial conditions obtained at $t = 0$ is solved. At $0 \leqslant t < t_*$, an equation similar to Eq. (16) can be written:

$$\int_S (\dot{W}_{,x} - \dot{\theta}y - \eta_{zx}^c)(\delta\dot{W})_{,x} + (\dot{W}_{,y} + \dot{\theta}x - \eta_{zy}^c)(\delta\dot{W})_{,y}\, dS = 0. \tag{22}$$

As Eq. (22) is integrated by parts, the following is obtained:

$$\int_C (\dot{W}_{,x} - \dot{\theta}y - \eta_{zx}^c)\, \delta\dot{W} n_x\, dC - \int_S \frac{\partial}{\partial x}(\dot{W}_{,x} - \eta_{zx}^c)\, \delta\dot{W}\, dS$$

$$+ \int_C (\dot{W}_{,y} + \dot{\theta}x - \eta_{zy}^c)\, \delta\dot{W} n_y\, dC - \int_S \frac{\partial}{\partial y}(\dot{W}_{,y} - \eta_{zy}^c)\, \delta\dot{W}\, dS = 0. \tag{23}$$

Equation (23) corresponds to the equilibrium equation (9) with the boundary conditions (10) [8]. As Eq. (22) is transformed, a system similar to system (20) is obtained:

$$[R^p](\dot{W}^p) = (\Phi^p). \tag{24}$$

Here $(\Phi^p) = s[B^p]^{\mathrm{t}}(\Psi^p)$ is the vector of right parts and $(\Psi^p) = (\dot{\theta}y_s + \eta_{zx_s}^c, -\dot{\theta}x_s + \eta_{zy_s}^c)^{\mathrm{t}}$.

Matrix $[R^p]$ in Eq. (24) coincides with the stiffness matrix in Eq. (20). Subscript s means that the values of the functions are determined at an integration point $L_1 = L_2 = L_3 = 1/3$. The time-dependent vector on the right side of Eq. (24) for the set of nodes is obtained by summing the right sides in the nodes of each element. At $0 \leqslant t < t_*$, the total stiffness matrix coincides with the matrix at $t = 0$ and is constant. With account for Eq. (7), it is possible to obtain expressions for stress rates in each element in matrix form. As a result of transformations, the following system of differential equations is obtained:

$$[R](\dot{W}) = (\Phi), \qquad (\dot{W}) = (\dot{W}^1, \dot{W}^2, \ldots, \dot{W}^{m_1})^{\mathrm{t}},$$

$$(\dot{\tau}_{zx}, \dot{\tau}_{zy})_p^{\mathrm{t}} = G([B^p](\dot{W}^p) - (\Psi^p)), \qquad p = 1, 2, \ldots, m_2. \tag{25}$$

Here m_2 is the number of elements in the system ($m_1 + 2m_2$ is the total number of equations in the system). System (25) is solved using the Runge–Kutta–Merson method [10]. Sufficiently fast convergence is ensured by the automatic control of the time step. When testing this method, the creep strains are first assumed to be zero, i.e., purely elastic deformation is considered in a time interval $0 \leqslant t < t_*$. As a result, the solution to system (25) for $\theta_0 = 0$ and $\dot{\theta} = \psi/t_* = \mathrm{const}$ coincides with the solution to system (21) for $\theta_0 = \psi$.

In order to invert matrix $[R]$ in solving a system of linear equations, the Fortran-based reflection method [11] is used. If damage is taken into account, m_2 differential equations should be added to system (25) to determine the damage parameter ω. It should be noted that the proposed solution method can be generalized to the case of orthotropy and different resistance of the material under tension and compression in the case of creep [12–15].
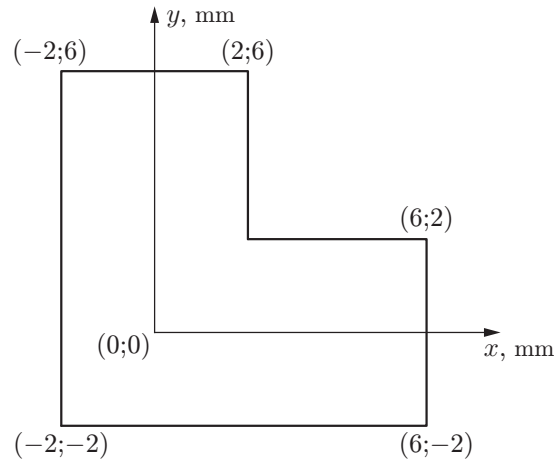
Fig. 1. Corner-shaped cross section.

Table 1. Results of solving direct problems for a rectangular rod

| Method	M_{z0}, N·m	$\dot{\theta} \cdot 10^3$, rad/(m·s)	M_{z*}, N·m	θ_{**}, rad/m
Finite element method	164.1	0 1.615	121.3 212.6	0.365 1.332
Finite difference method	163.7	0 1.615	121.4 212.5	0.361 1.330

3. EXAMPLES OF SOLUTIONS TO THE PROBLEMS

The calculation is carried out for (10×20)-mm rectangular rods and corner-shaped rods with a angle between the flanges equal to $90°$ (Fig. 1). The calculations are performed for the VT9 alloy with no account for damage accumulation using dependences and parameters in Eq. (8) corresponding to a temperature $T = 550°$C: $f_1(\sigma_i) = B_1\sigma_i^n$ and $f_2(\sigma_i) = B_2\sigma_i^g$, where $n = 4$, $g = 5$, $m = 10$, $B_1 = 1.1303 \cdot 10^{-17}$ MPa^{-n}·s^{-1}, and $B_2 = 5.0105 \cdot 10^{-20}$ MPa^{-g}·s^{-1} [16]. Young's modulus is $E = 66\,700$ MPa, Poisson's coefficient is $\nu = 0.3$, and yield strength is $\sigma_{\text{t}} = 608$ MPa.

3.1. Direct Problems for a Rectangular Rod

The section is partitioned by a $m_1 = 861$ node (21 along the x axis and 41 along the y axis with a step of 0.5 mm) into $m_2 = 1600$ elements. Table 1 shows the problem solution results [the initial moment M_{z0} calculated according to Eq. (6), the moment before unloading M_{z*}, and the residual angle θ_{**}] with no account for the damage parameter [$m = 0$ in Eq. (8)] for the relaxation mode ($\dot{\theta} = 0$) and the mode with a constant angular twist rate [$\dot{\theta} = 1.615 \cdot 10^{-4}$ rad/(m·s)]. The given time is $t_* = 1.08 \cdot 10^4$ s and the initial linear angle at $t = 0$ is $\theta_0 = 1.396$ rad/m. Table 1 also shows the solution of the same problems by the finite difference method [1] with an 0.5-mm step along the x and y axes. At $t = 0$, the difference in the computational results for the moments is smaller than 0.3%; at $t = t_*$, it is less than 0.1% and the residual twist angles differ by less than 1.1%.

3.2. Inverse Problems for a Rectangular Rod

Figure 2a shows the dependence of the initial angle on time for the values of the residual angle $\theta_{**} = 0.175$, 0.349, and 0.524 rad in the case of deformation relaxation ($\dot{\theta} = 0$) at $t_* = 7.2 \cdot 10^3$–$3.6 \cdot 10^6$ s. Figure 2b shows the same dependence for $t_* \approx 7.2 \cdot 10^3$–$7.2 \cdot 10^4$ s. Depending on the initial data, about 8–15 iterations k are needed to ensure the accuracy of the iteration process (13) and (14) $(\theta_{**} - \theta_{**}^k)/\theta_{**} \leqslant 10^{-4}$.
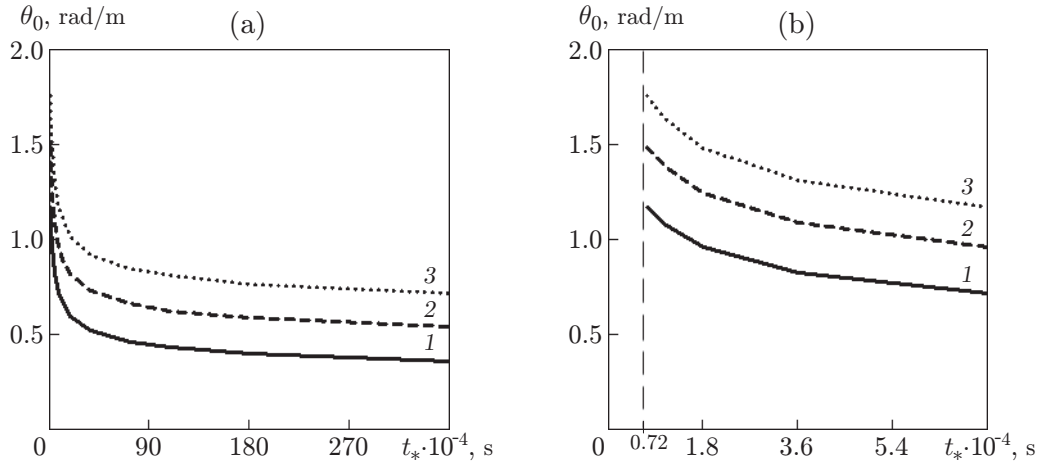
Fig. 2. Initial angle versus time $\theta_0(t_*)$ for the deformation relaxation within ranges $t_* = 7.2 \cdot 10^3$ to $3.6 \cdot 10^6$ s (a) and $t_* = 7.2 \cdot 10^3$ to $7.2 \cdot 10^4$ s (b) for $\theta_{**} = 0.175$ (*1*), 0.349 (*2*), and 0.524 rad (*3*).
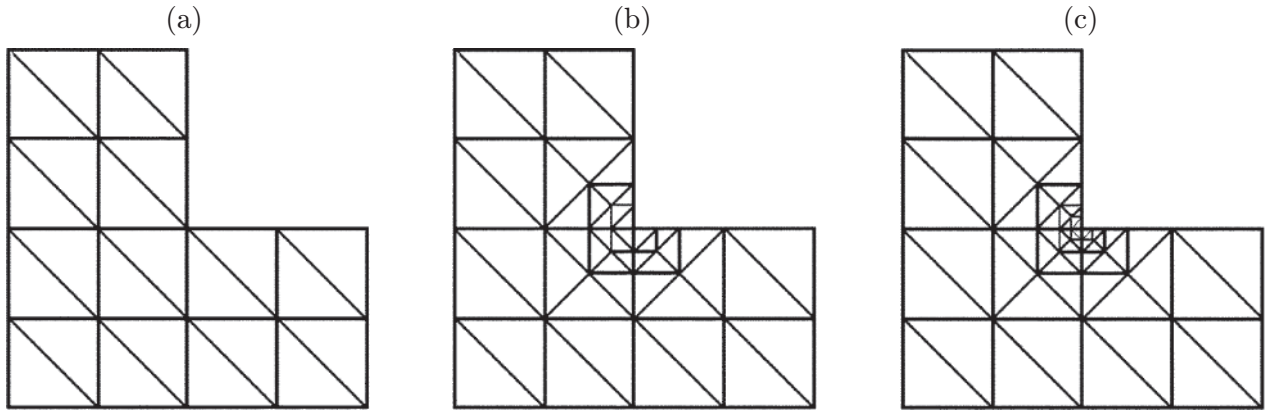
Fig. 3. Partition of the corner-shaped cross section: uniform partition (a) and nonuniform partition with an additional number of nodes 14 (b) and 21 (c) in the stress concentration region.

Table 2. Results of solving the direct problem for a corner-shaped rod

$h \cdot 10^3$, m	Partition type	M_{z0}, N·m	M_{z*}, N·m	θ_{**}, rad/m	$\sigma_{i0\,max}$, MPa
0.2	Fig. 3a	5.420	4.826	0.1030	342.7
0.2	Fig. 3b	5.410	4.831	0.1033	594.9
0.5	Fig. 3a	5.504	4.951	0.1028	253.7
1.0	Fig. 3a	5.703	5.098	0.1018	199.3
1.0	Fig. 3b	5.578	4.969	0.1048	352.4
1.0	Fig. 3c	5.567	4.963	0.1042	442.1

897
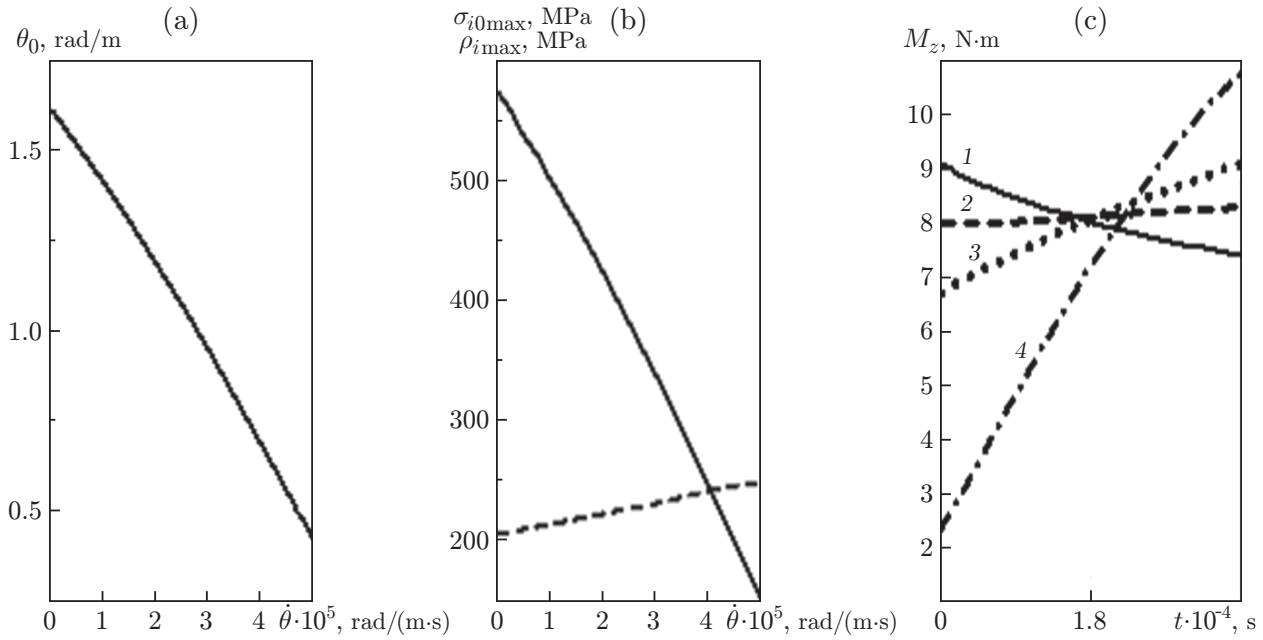
Fig. 4. Solution of the inverse problem for a corner-shaped rod ($t_* = 3.6 \cdot 10^4$ s and $\theta_{**} = 0.3$ rad/m): (a) dependence θ_0 on $\dot{\theta}$; (b) dependences of the maximum stress intensity in the section $\sigma_{i0\,max}(\dot{\theta})$ at $t = 0$ (solid curve) and $\rho_{i\,max}(\dot{\theta})$ at $t = t_*$ after unloading (dashed curve); (c) torque versus time at $\dot{\theta} = 0$ (*1*), 10^{-5} (*2*), $2 \cdot 10^{-5}$ (*3*), and $5 \cdot 10^{-5}$ rad/(m·s) (*4*).

3.3. Direct Problems for a Corner-Shaped Rod

The special feature of a corner-shaped rod is that it has a point whose vicinity is a stress concentration region. The stresses in this region tend to infinity. If such regions are present, it is difficult to use the finite difference method for calculations. Therefore, the solution is obtained using the finite element method.

It is revealed how the type of a finite element grid affects computational results. The section is subjected to uniform partition (Fig. 3a) with equal steps along the x and y axes and nonuniform partition, which is denser in the stress concentration region (Figs. 3b and 3c). The results of the solution of the direct problem of torsion with an initial twist angle $\theta_0 = 0.95$ rad/m and $t_* = 7.2 \cdot 10^4$ s for partitions of various types are given in Table 2. In the case of fine partition, in which case the step along the x and y axes is $h = 0.2$ mm and corresponds to Fig. 3a, the total numbers of nodes and elements are $m_1 = 1281$ and $m_2 = 2400$, respectively. In the case of nonuniform partitioned (Fig. 3b), we have $m_1 = 1295$ and $m_2 = 2424$. The maximum stress intensity values obtained with account for Eq. (12) before unloading are $\sigma_{i*} = 197.4$ MPa and $\sigma_{i*} = 234.1$ MPa, respectively.

It follows from Table 2 that, despite the significant difference in the stress intensity in the concentration regions for uniform and nonuniform partition, the resulting values of the moments at the initial time M_{z0} and before elastic unloading M_{z*} differ insignificantly. Moreover, with a decreasing grid step h, the convergence of these integral values is observed. The difference in the values of the residual twist angles θ_{**} does not exceed 0.5%. Thus, uniform partition can be used for the calculations with satisfactory accuracy. Stresses in the stress concentration regions are usually reduced by rounding in the flange joint zones, and plastic deformations are also taken into account [17].

3.4. Inverse Problem of Pure Torsion of a Corner-Shaped Rod

Figure 4 presents the results of the finite element solution to the problem of determining angle θ_0, necessary to obtain the residual angle $\theta_{**} = 0.3$ rad/m, for various creep modes $\dot{\theta} = $ const within a time interval $0 \leqslant t < t_*$ ($t_* = 3.6 \cdot 10^4$ s). The calculations are based on the uniform partition with a step $h = 0.2$ mm. Figure 4a shows

898
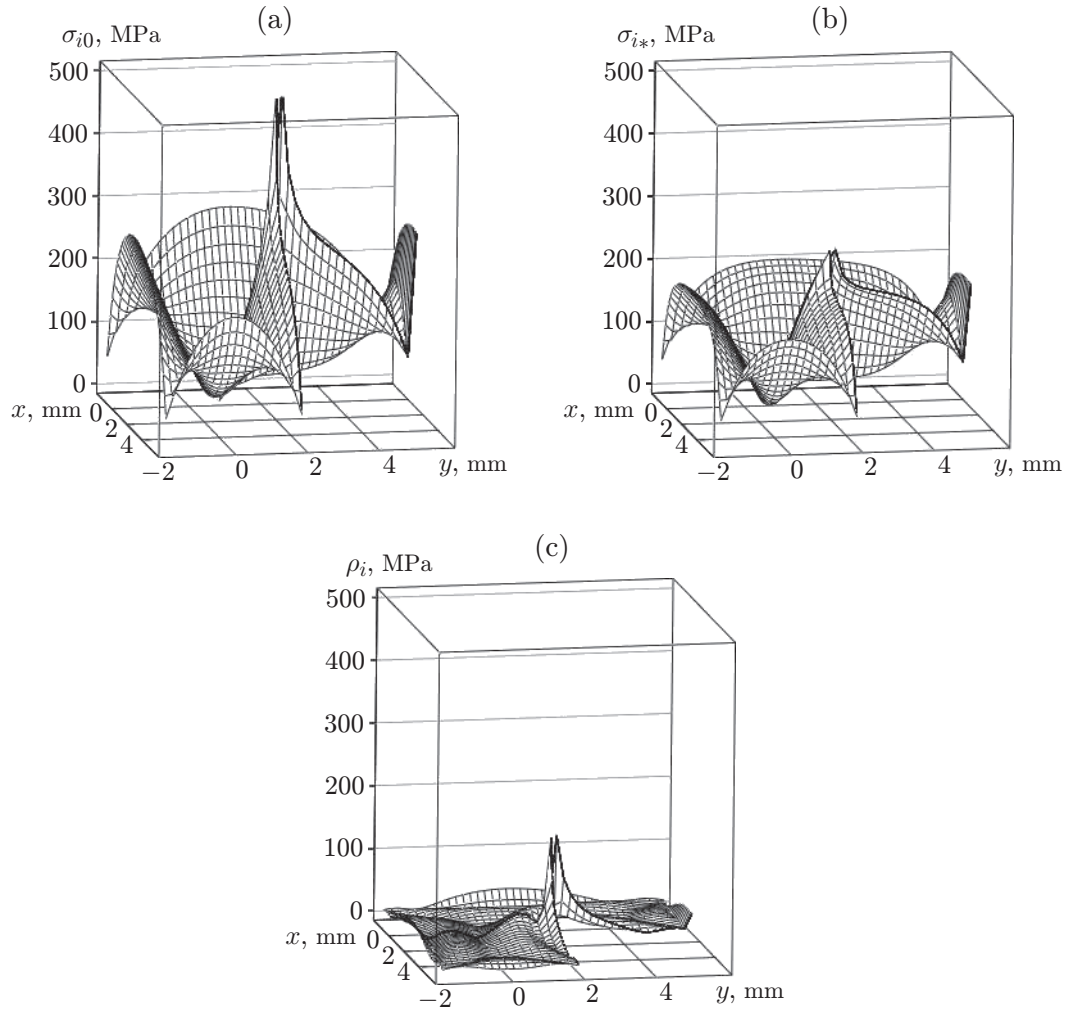
Fig. 5. Stress intensity surface in the corner-shaped rod in the case of deformation relaxation $\dot{\theta} = 0$ for $t = 0$ (a) and $t = t_*$ before unloading (b) and after unloading (c).

the desired angle θ_0 as a function of the twist angle rate $\dot{\theta}$; Fig. 4b shows the dependences of the maximum stress intensity in the section on the angular twist rate $\dot{\theta}$. The minimum value of residual stresses is observed during the deformation relaxation ($\dot{\theta} = 0$), which confirms the results obtained in [2]. For curves shown in Fig. 4c, the initial twist angle is determined from the curve illustrated in Fig. 4a. Mode 2 $[\dot{\theta} = 10^{-5} \text{ rad}/(\text{m} \cdot \text{s})]$ is close to the constant torque mode.

Figure 5 shows the stress intensity surface in the corner-shaped rod. For comparison, Fig. 6 shows the same surface for different modes $\dot{\theta} = \text{const}$ in profile projection.

The analysis of the surfaces shown in Fig. 6 allows for the following conclusions. Despite the fact that the residual stresses during the deformation relaxation are the smallest (Figs. 6a–6c), the initial stresses ($t = 0$) are the largest. This can lead to significant damage and even destruction of the structure during torsion. The modes where $\dot{\theta} = 2 \cdot 10^{-5}$ and $5 \cdot 10^{-5} \text{ rad}/(\text{m} \cdot \text{s})$ (see Figs. 6g–6l) contribute to a significant decrease in the stress intensity in the stress concentration region. It is also noteworthy that the VT9 alloy is described by the energy version of the creep theory, when the dissipation work is a constant value [7]. The parameters of this alloy satisfy the condition $g > n$, so the lowest level of damage accumulation is observed when the twist angle linearly changes during deformation [5]. The closest to this deformation mode is the mode where $\dot{\theta} = 5 \cdot 10^{-5} \text{ rad}/(\text{m} \cdot \text{s})$ (Figs. 6j–6l).
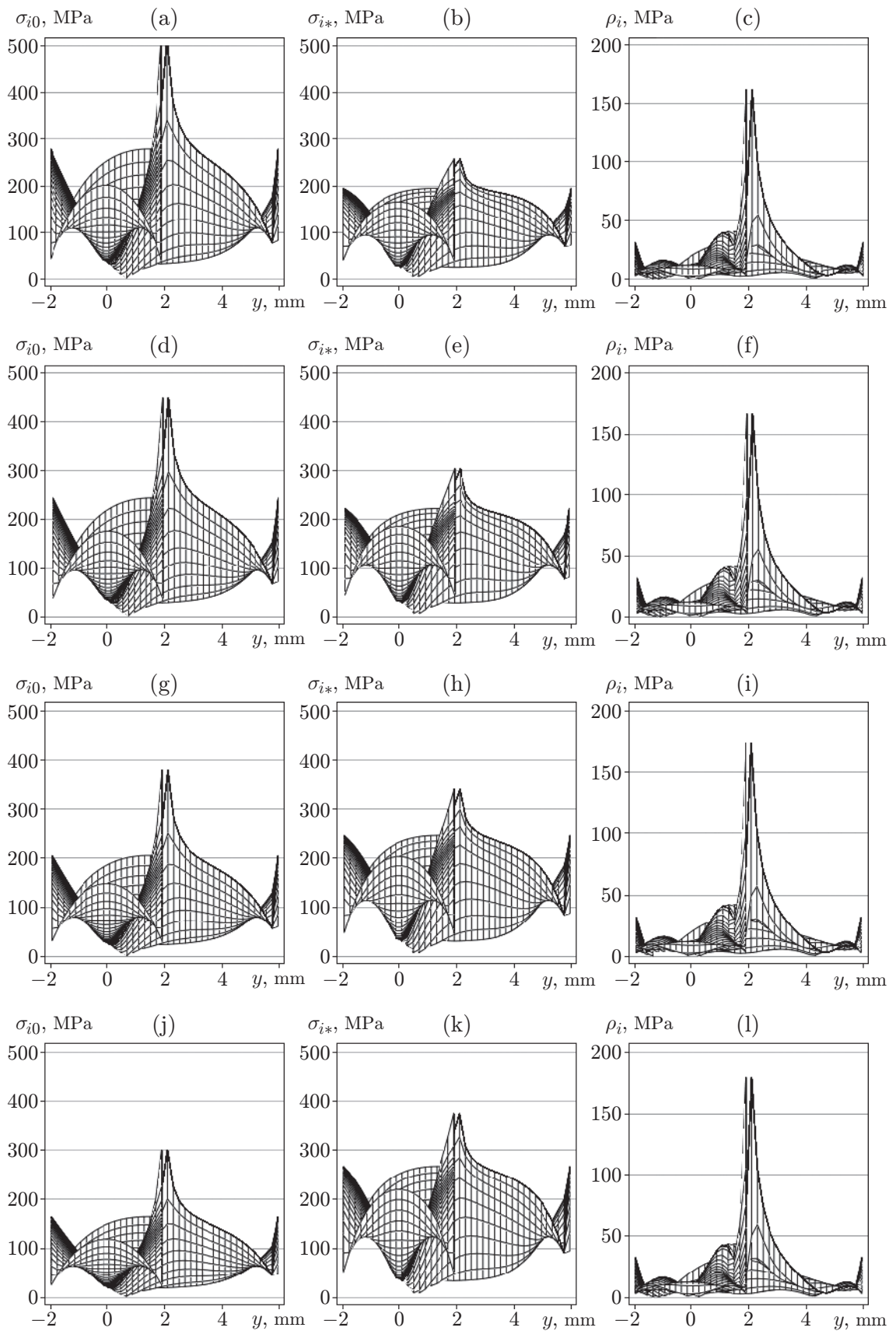
Fig. 6. Profile projection of the stress intensity surface in the corner-shaped rod for $\dot{\theta} = 0$ (a–c), 10^{-5} (d–f), $2 \cdot 10^{-5}$ (g–i), and $5 \cdot 10^{-5}$ rad/(m·s) (j–l) at $t = 0$ (a, d, g, and j), $t = t_*$ (before unloading) (b, e, h, and k), and $t = t_*$ (after unloading) (c, f, i, and l).

CONCLUSIONS

This paper considers direct and inverse problems of torsion of rectangular and corner-shaped rods in creep modes, where the angular twist rate is assumed to be given during deformation. For the section being formed, a constant linear twist angle is set and there is no constraint on the ends of the rod. This condition allows reducing this problem to a two-dimensional problem in the cross-sectional plane of the rod. After the completion of the molding process within a predetermined time, elastic recovery occurs as a result of the unloading. A technique for numerical calculation using the finite element method is developed. The proposed method makes it possible to obtain the stiffness characteristics of the section under torsion in the case of creep. It is revealed how the density of uniform and nonuniform finite element partition in the stress concentration region affects the computational results. It is shown numerically that the lowest residual stresses are observed during the deformation relaxation. The influence of the deformation mode on the stress concentration in a corner-shaped rod is investigated.

REFERENCES

1. I. A. Banshchikova, B. V. Gorev, and I. V. Sukhorukov, "Two-Dimensional Problems of Beam Forming under Conditions of Creep," Prikl. Mekh. Tekh. Fiz. **43** (3), 129–139 (2002) [J. Appl. Mech. Tech. Phys. **43** (3), 448–456 (2002); https://doi.org/10.1023/A:1015382723827].

2. I. A. Banshchikova and I. Yu. Tsvelodub, "On One Class of Inverse Problems of Variation in Shape of Viscoelastic Plates," Prikl. Mekh. Tekh. Fiz. **37** (6), 122–131 (1996) [J. Appl. Mech. Tech. Phys. **37** (6), 876–883 (1996); https://doi.org/10.1007/BF02369267].

3. K. S. Bormotin and N. A. Taranukha, "Mathematical Modeling of Inverse Problems of Forming Taking into Account the Incomplete Reversibility of Creep Strain," Prikl. Mekh. Tekh. Fiz. **59** (1), 161–171 (2018) [J. Appl. Mech. Tech. Phys. **59** (1), 138–145 (2018); https://doi.org/10.1134/S0021894418010170].

4. K. S. Bormotin, "Inverse Problems of Optimal Control in Creep Theory," Sib. Zh. Indust. Mat. **15** (2), 33–42 (2012) [J. Appl. Ind. Math. **6** (4), 421–430 (2012); https://doi.org/10.1134/S1990478912040035].

5. I. Yu. Tsvelodub, *Postulate of Stability and Its Applications in the Theory of Creep of Metallic Materials* (Lavrentyev Inst. of Hydrodynamics, Sib. Branch, Acad. of Sci. of the USSR, Novosibirsk, 1991) [in Russian].

6. I. A. Birger, *Rods, Plates, and Shells* (Fizmatlit, Moscow, 1992) [in Russian].

7. B. V. Gorev, I. V. Lyubashevskaya, V. A. Panamarev, and S. V. Iyavoynen, "Description of Creep and Fracture of Modern Construction Materials Using Kinetic Equations in Energy Form," Prikl. Mekh. Tekh. Fiz. **55** (6), 132–144 (2014) [J. Appl. Mech. Tech. Phys. **55** (6), 1020–1030 (2014); https://doi.org/10.1134/S0021894414060145].

8. O. C. Zienkiewicz, *The Finite Element Method in Engineering Science* (McGraw-Hill, London, 1971).

9. V. I. Myachenkov, V. P. Mal'tsev, V. P. Maiboroda, et al., *Calculations of Machine-Building Structures by the Finite Element Method* (Mashinostroenie, Moscow, 1989) [in Russian].

10. A. E. Mudrov, *Numerical Methods for PC in BASIC, Fortran, and Pascal* (MP RASKO, Tomsk, 1991) [in Russian].

11. A. N. Konovalov, *Introduction to the Computational Methods of Linear Algebra* (Nauka, Novosibirsk, 1993) [in Russian].

12. I. A. Banshchikova, I. Yu. Tsvelodub, and D. M. Petrov, "Deformation of Structural Elements Made of Alloys with Reduced Resistance to Creep in Shear Direction," Uch. Zap. Kazan. Univ., Ser. Fiz.-Mat. Nauki **157** (3), 34–41 (2015).

13. I. A. Banshchikova and A. Yu. Larichkin, "Torsion of Solid Rods with Account for the Different Resistance of the Material to Tension and Compression under Creep," Prikl. Mekh. Tekh. Fiz. **59** (6), 123–134 (2018) [J. Appl. Mech. Tech. Phys. **59** (6), 1067–1077 (2018); https://doi.org/10.1134/S0021894418060123].

14. I. A. Banshchikova, "Construction of Constitutive Equations for Orthotropic Materials with Different Properties in Tension and Compression under Creep Conditions," Prikl. Mekh. Tekh. Fiz. **61** (1), 102–117 (2020) [J. Appl. Mech. Tech. Phys. **61** (1), 87–100 (2020); https://doi.org/10.1134/S0021894420010101].

15. I. A. Banshchikova, D. M. Petrov, and I. Yu. Tsvelodub, "Torsion of Circular Rods at Anisotropic Creep," J. Phys.: Conf. Ser. **722** (1), 012004 (2016).

16. A. F. Nikitenko and I. V. Sukhorukov, "Approximate Method for Solving Relaxation Problems in Terms of Material's Damagability under Creep," Prikl. Mekh. Tekh. Fiz. **35** (5), 136–142 (1994) [J. Appl. Mech. Tech. Phys. **35** (5), 770–775 (1994); https://doi.org/10.1007/BF02369559].

17. R. R. Mavlyutin, *Stress Concentration in Aircraft Structural Elements* (Nauka, Moscow, 1981) [in Russian].